JOURNAL OF PURE AND APPLIED MICROBIOLOGY, April 2013. Vol. **7**(Spl. Edn.), p. 269-276

A Cerebral Autoregulation Simulator based on the Model of Intracranial Dynamics

Shyan-Lung Lin*, Hua-Wei Lin and Hsing-Cheng Chang

Department of Automatic Control Engineering, Feng Chia University, Taiwan.

(Received: 03 March 2013; accepted: 14 April 2013)

Cerebral Autoregulation (CA) maintains a steady cerebral blood flow within a normal range regardless the variations of blood pressure and other bio-information. CA is a phenomenon describing automatic cerebral regulation to maintain a steady cerebral blood flow (CBF), or cerebral blood volume (CBV). Studies of CA modeling may involve with cerebral hemodynamics, intracranial hemodynamics, CSF dynamics, and ICP dynamics.In this paper, we employed the electric analog of intracranial dynamics to implement the CA simulator with Matlab platform. The model of the arterial-arteriolar cerebrovascular bed was proposed by Ursino with description of blood dynamics and biomechanics from the viewpoints of both cerebral circulation and intracranial space. With the fulfillment of this CA simulator, we can successfully the dynamics of blood vessels in brain subject to possible variations toward cerebral autoregulation. We demonstrated the CA relations of wall thickness vs. radius of artery, hydraulic conductance vs. radius of artery, blood volume vs. radius of artery, elastic stress vs. radius of artery, smooth muscle tension vs. radius of artery, middle cerebral artery vs. transmural pressure, and temporal responses of artery radius and cerebral blood flow.

Key words: Cerebral autoregulation, intracranial dynamics, cerebrovascular bed, simulator.

Lassen[1] was first to propose the concept of CA in which CBF maintains a steady value when cerebral perfusion pressure (CPP) or mean arterial pressure (MAP) changes within approximately 50 to 160 mmHg [2-3]. Cerebral autoregulation is effected through the control the smooth muscle of the artery to alter the arterial vascular diameter regulating cerebral blood flow volume and the CBF autoregulation curve will be changed by hypercapnia and sympathetic nervous stimulus. CA can be divided into static and dynamic. As static autoregulation is the overall efficiency of measuring a change in blood pressure over a long period of time, dynamic autoregulation, meanwhile, is the CBF remaining steady with short-term blood pressure changes]. Dynamic and static have been confirmed for two different types of mechanisms, Dawson *et al*. [5] also found that the dynamic mechanism is more involved in cerebral vascular disease.

Since the cerebral hemodynamics, CSF and ICP dynamics, intracranial hemodynamics and hydrodynamics, activity of metabolism and gas transportation are necessarily involved,the correlation and interaction of physiological systems associated with the CA mechanism are extremely complex and fascinating. CA mechanism rely on the techniques of linear/nonlinear analysis, time/

* To whom all correspondence should be addressed.
E-mail: sllin@fcu.edu.tw

frequency domain analysis, transient/steady state analysis of the interactions among human pressure properties, heart rate signals, and gas activities. To compare the results of intact and impaired autoregulatory capacity in humans, Tiecks *et al.*[4] used the model based on second order linear ordinary differential equations, similar to a harmonic oscillator, and concluded that measurement of dynamic autoregulation results in normal human is similar to the static testing of intact and pharmacologically impaired results. The analogy electric analog [6]was also used to model the brain regulatory mechanisms, which takes into account the preservation of the brain cavity capacity, aorta, and cerebral vascular and cortical vein.

In Ursino's pioneer works7-8, a model of intracranial hydrodynamics was proposed under the constancy of overall intracranial volume. The model was able to simulate the behavior of intracranial arterial vascular bed, intracranial venous vascular bed, cerebrospinal fluid (CSF) absorption and production processes. Ursino *et al.*,[9-10] laterproposed another model, which depicts the production and diffusion of vasoactive chemical factors involved in oxygen-dependent CBF regulation, and the simulation results suggested that chemical factors, adenosine and H^+, play a significant but not exclusive role in the regulation of the cerebral vascular bed.

Ursino[11] modeled the CA into electric analog of intracranial dynamics with description of blood dynamics and biomechanics, modeling. Based on two different viewpoints of cerebral circulation and intracranial space, the model also studied the CSF dynamics, CA, and carbon dioxide reactivity. Again, Ursino *et al.*,[12] used the Windkessel model to represent the part of circulation and simplified the previously model[11]. A revised model of cerebrovascular regulation, in which focal point is taken into account to the role of tissue hypoxia on CBF, was later proposed[12] to successfully explain the increase in CBF and the vasoconstriction of small pial arteries during hemodilution, attributing to the decrease of blood viscosity and the antagonistic action of the flow-dependent mechanism (responsible for vasoconstriction) and of hypoxia (responsible for vasodilation).

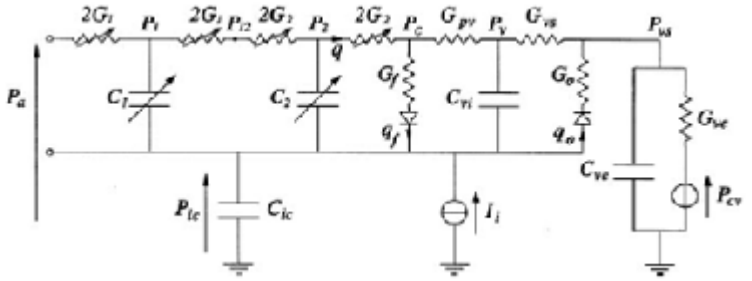

G_1 and C_1 : hydraulic conductance and compliance of the proximal arterial cerebrovascularbed (basal brain arteries and large pial arteries), respectively;
G_2 and C_2: hydraulic conductance and compliance of the distal arterial cerebrovascular bed (medium and small pial arteries), respectively;
C_{ic}: intracranial tissue compliance;
C_{vi}: intracranial venous compliance;
G_{pv}: hydraulic conductance of the proximal venous cerebrovascular bed;
G_{vs}: hydraulic conductance of the distal venous cerebrovascular bed (lateral lacunae and bridge veins);
G_f: CSF formation conductance;
G_o: CSF outflow conductance;
G_{ve} and C_{ve}: hydraulic conductance and compliance of the extracranial venous pathways;
P_a: arterial pressure;
P_1 : average intravascular pressure in the proximal (arterial) cerebrovascular bed;
P_2: average intravascular pressure in the distal (arteriolar) cerebrovascular bed;
P_c: capillary pressure;
P_v: cerebral venous pressure;
P_{vs}: dural sinus pressure; P_{ic}: intracranial pressure;
P_{cv}: central venous pressure

Fig. 1. The electric analog of intracranial dynamics by Ursino [11]

Some successful simulators have been implemented lately by researchers in distinct fields[13-14]. Although numerous researchers were devoted into the study of CA models[15-16], little accomplishment was found in the implementation of CA simulation tool. Giannessi *et al*.,[17] exploited previously developed CBF and ICP model to simulate the interaction in cerebrovascular dynamics. In current study, we employed the model of the arterial-arteriolar cerebrovascular bed proposed by Ursino[11] to implement a numerical computation process and simulator based on Matlab.

The mathematical model

Cerebral circulation occurs in a sealed space (skull and craniospinal axis). Any variation in vascular caliber may affect ICP through alters of CBV. ICP is the extravascular pressure of cerebral vascular and is always slightly higher than the pressure in large cerebral veins. Any excessive change of ICP can cause a significant impact on cerebral hemodynamics.

The Ursino's model[11] can be applied to a vast range of situations, and also involves with the interaction among CA, ICP and CBV changes. Circuit components in the electric analog of intracranial dynamics (Figure 1) include: G_1 and C_1, hydraulic conductance and compliance (proximal cerebral arteries); G_2 and C_2, hydraulic conductance and compliance (distal cerebral arteries); P_a, systemic arterial pressure (SAP); P_1 and P_2, intravascular pressure of large pial arteries and medium and small arteries; q, cerebral blood flow (CBF); P_c and P_v, capillary and cerebral venous pressure; P_{vs} and P_{cv}, sinus venous and central venous pressure; P_{ic}, intracranial pressure (ICP); C_{ic}, intracranial compliance; G_{pv} and C_{vi}, hydraulic conductance and compliance of large cerebral veins; G_{vs}, hydraulic conductance of terminal intracranial veins; G_{ve} and C_{ve}, hydraulic conductance and compliance, of extracranial venous pathways; G_f and G_o, conductance to CSF formation and outflow; q_f and q_o, rates of CSF formation and outflow; and I_i, artificial CSF injection rate.

Arterial-Arteriolar Cerebrovascular Bed

The cerebrovascular bed divided into two sections is justified by the heterogeneity of cerebrovascular regulation: the proximal segment is large pial arteries and the distal segment is small pial arteries. The change of blood volume and conductance can be calculated by simulating each segment vascular with the intravascular radius. According to the Hagen-Poiseuille law, the blood volume (V) is proportional to the second power of the intravascular radius (r), and the conductance (G) is proportional to the fourth power of the intravascular radius (r).

$$G_j = K_{G,j} r_j^4 \qquad j = 1,2 \quad (1)$$

$$V_j = K_{v,j} r_j^2 j = 1,2 \quad (2)$$

$$P_j r_j - P_{ic}(r_j + h_j) = T_{e,j} + T_{m,j} + T_{v,j} = T \qquad j = 1,2 \quad (3)$$

where K_G is set to obtain a physiological pressure drop in basal condition. K_V isset to obtain physiological values of blood volume in each segment. r_j is the intravascular radius of the corresponding blood vessels, P is the intravascular pressure in the jth segment; P_{ic} is the intracranial pressure; h_j is wall thickness; and $T_{e,j}$ is elastictension, $T_{m,j}$ is smooth muscle tension, $T_{v,j}$ is viscous tension.

Elastic stress (T_e) increases exponentially with the intravascular radius (r), reflecting the behavior of elastin and collagen fibers in the wall.

$$T_{e,j} = \sigma_{e,j} h_j \qquad j = 1,2 \quad (4)$$

$$\sigma_{e,j} = \sigma_{e0,j}\left[\exp\left(K_{T,j}\cdot\frac{r_j - r_{0j}}{r_{0j}}\right) - 1\right] \quad \sigma_{e,j} < \sigma_{coll,j} \qquad j = 1,2 \quad (5)$$

where σ_e is elastic stress (force per unit surface), r_0 is the inner radius in unstressed wall. σ_{coll} is introduced to permit the vascular tosupport a mediumnegative tension before collapsing.

Smooth muscle tension T_m depends on the intravascular radius through a campanular relationship, which reflects the different overlapping of actin and myosin filaments. Smooth muscle tension increases to maximum at a particular optimal value of intravascular radius and then progressively decreases.

$$T_{m,j} = T_{max,j} \cdot \exp\left\{-\left|\frac{r_j - r_{m,j}}{r_{t,j} - r_{m,j}}\right|^{n_{m,j}}\right\} \qquad j = 1,2 \quad ...(6)$$

where r_m is the optimal radius at which smooth muscle exerts maximal force; T_{max} is the corresponding active tension; r_t and n_m are constant parameters used to represent the appropriate shape of the campanular relationship. Viscous tensions (T_v) in intravascular radius (r)

can be calculated by the following equations:

$$T_{v,j} = \sigma_{v,j} h_j \qquad j = 1,2 \qquad ...(7)$$

$$\sigma_{v,j} = \frac{\eta_j}{r_{c,j}} \left(\frac{dr_j}{dt} \right) \qquad j = 1,2 \qquad ...(8)$$

where σ_v (force per unit length)denotes a linear dependency on the time derivative of wall strain;$\eta_j$denotes wall viscosity.

Wall thickness (h) can be calculated of the intravascular radius (r), by assuming that the vascular wall is incompressible; therefore, the vascular volume maintains constant. Mathematical expressions for tensions have been given to reproduce results of experimental studies on isolated arterioles (Davis, *et al*. 1989).

$$h_j = -r_j + \sqrt{r_j^2 + 2r_{c,j} h_{w,j} + h_{w,j}^2} \qquad j = 1,2 \qquad ...(9)$$

CBF (q) can be calculated of pressure drop and conductance in any longitudinal segment. When calculating CBF, the CSF circulation can be negligible.

$$q = 2G_2 (P_2 - P_c) \qquad ...(10)$$

CSF Dynamics and Intracranial Hemodynamics

The main biomechanical law at the basis of intracranial dynamics is the constancy of the overall volume contained in the craniospinal space. Any volume change in intracranial space will cause a compression or dislocation of the remaining volumes, along with the variation in ICP (Pic). The phenomenon is mathematically reproduced by means of intracranial compliance (C_{ic}). Assumed that the quantity is inversely proportional to ICP through a constant parameter (k_E) called the elastance coefficient.

$$C_{ic} = \frac{1}{k_E P_{ic}} \qquad ...(11)$$

Cerebral Venous Circulation

The venous compliance (C_{vi}) is inversely dependent on transmural pressure, signifying a mono-exponential pressure-volume relationship.

$$C_{vi} = \frac{1}{\tau_{vi0} (P_v - P_{ic} - P_{vi})} \qquad ...(12)$$

The conductance values (G_{pv} and G_{vs}) of intracranial veins can be calculated by assuming that the intracranial venous circulation as a Starling resistor[19]. The conductance of the terminal veins (G_{vs}) is considered to rely on pressures through the following equation.

$$G_{vs} = G'_{vs} \left(\frac{P_v - P_{ic}}{P_v - P_{vs}} \right) \qquad ...(13)$$

The CSF Production and Absorption Mechanisms

CSF Production

It is thought that CSF originates at the choroid plexi of the lateral ventricles through an active or energy requiring process. Nevertheless, evidence that the CSF production rate (q_f) decreases by increasing the ICP (P_{ic}) or decreasing the CBF (q) has been reported.

$$q_f = \frac{P_c - P_{ic}}{R_f} \qquad ...(14)$$

where is proportional to the transmural pressure at the choroid capillary level, denotes the resistance that the choroid capillary system offers to CSF secretion, means capillary pressure; means intracranial pressure.

CSF Reabsorption

The process by which CSF is reabsorbed by the arachnoid villi of the sagittal sinus and other minor routes seems to be purely passive, depending on the difference between CSF pressure and dural sinus pressure and on the resistance that the arachnoid villi offer to liquid outflow.

$$q_a = \frac{P_{ic} - P_{vs}}{R_a} \qquad ...(15)$$

where is the rate of CSF absorption, the venous sinus pressure and the resistance to CSF outflow.

MCA (middle cerebral artery)

The behaviour of MCA is essentially passive in nature. The intravascular radius of MCA (V_{MCA}) is calculated as a function of transmural pressure (P_a - P_{ic}), assuming a mono-exponential pressure-radius relationship. The is therefore a logarithmic function of transmural pressure,

$$r_{MCA} = r_{MCA0} \left[\frac{1}{K_{MCA}} \cdot \ln \left(\frac{P_a - P_{ic}}{P_{a0} - P_{ic0}} \right) + 1 \right] \qquad ...(16)$$

where is a constant parameter and denotes the inner radius in basal condition.

Blood velocity in MCA (V_{MCA}) can be calculated as the ratio of CBF and cross-sectional

area. Assume that about one-third of total CBF passes through each MCA. Due to these assumptions, the basal value of is 60 cm/s (normally is 33~90 cm/s, averaged is 62 cm/s).

$$V_{MCA} = \frac{q}{3}\left(\frac{\cdot}{\cdot_{MCA}}\right) \quad ...(17)$$

RESULTS AND DISCUSSION

The simulator of the CA is based on Matlab. Figure 2 shows the Matlab simulation interface. The interface incorporates seven different simulation environments for different needs. Meanwhile, each of the seven different simulation environments also includes another two or three different blocks. Users may utilize the simulation interface options to select different blocks, and then enter different parameters to adjust the interface and obtain different graphical output.

As is depicted in Fig. 2, the simulator provides 7 functional modules for simulations of CA responses:

1. Simulation of wall thickness (h) vs. radius of artery (r)
2. Simulation of hydraulic conductance (G) vs. radius of artery (r)
3. Simulation of blood volume (V) vs. radius of artery (r)
4. Simulation of elastic stress (T_e) vs. radius of artery (r)
5. Simulation of smooth muscle tension (T_m) vs. radius of artery (r)
6. . Simulation of middle cerebral artery (MCA) vs. transmural pressure (P_a-P_{ic})
7. Simulation of temporal responses of artery radius (r(t)) and cerebral blood flow (q(t))

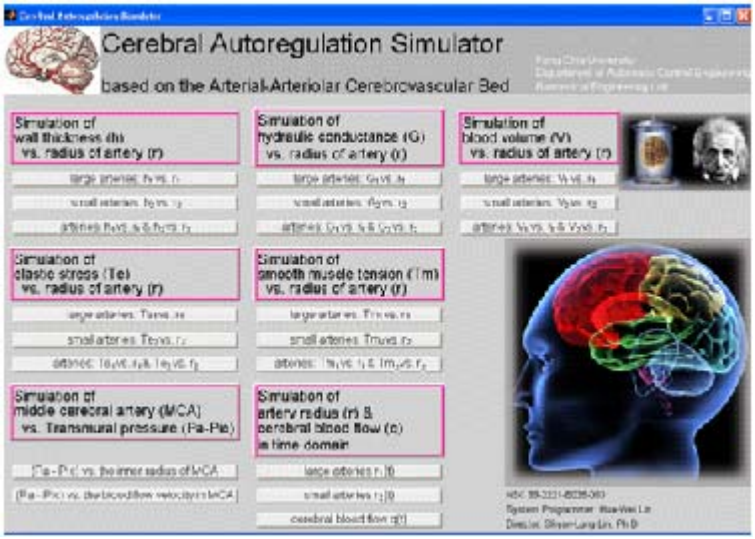

Fig. 2. The CA simulator implemented with Matlab

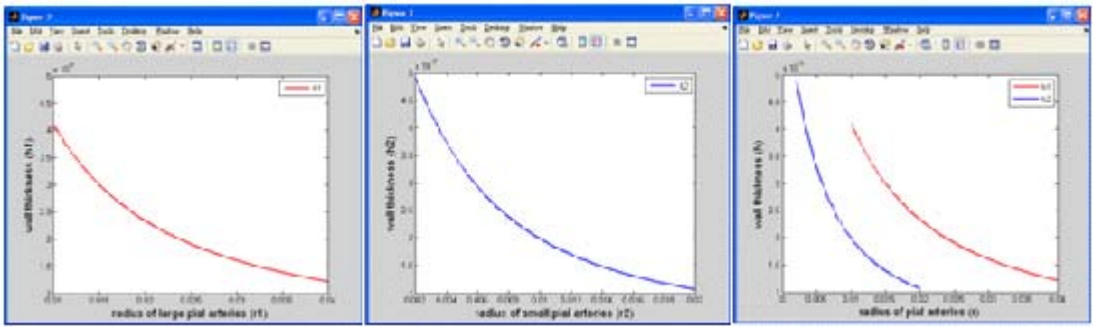

Fig. 3. Simulation of wall thickness (h_1 and h_2) vs. radius of large and small pial arteries (r_1 and r_2)

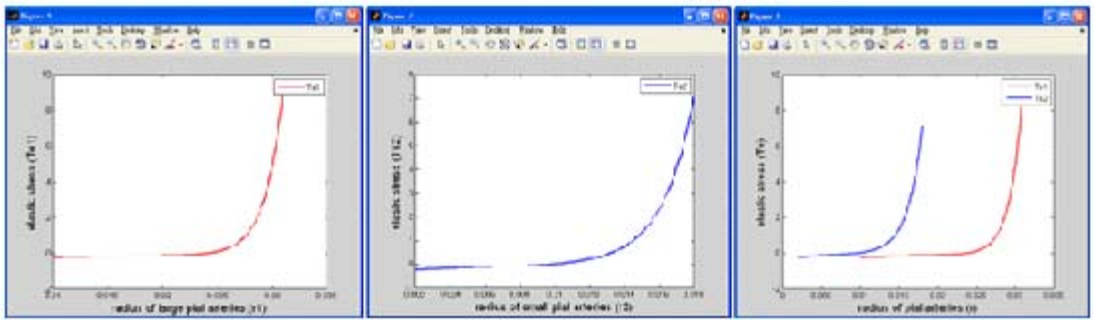

Fig. 4. Simulation of elastic stress (Te_1 and Te_2) vs. radius of large and small pial arteries (r_1 and r_2)

In Fig. 4, we show the simulation results of the simulation module 4 with following initial parameters: r_{01}=0.015 (cm), h_{01}=0.003 (cm), σ_{e1}=0.1425 (mmHg), $\sigma_{coll,1}$=62.79 (mmHg), r_{02}=0.0075 (cm), h_{02}=0.0025 (cm)0$\sigma_{e,2}$=11.19 (mmHg), $\sigma_{coll,2}$=41.32 (mmHg). The responses of T_{e1} (elastic tension) vs. r_1 and T_{e2} (elastic tension) vs. r_2 are shown in the left and middle portions of Fig. 4, respectively. In the right portion of Fig. 4, both elastic tension and radius of large and small pial arteries, (T_{e1} vs. r_1) and (T_{e2} vs. r_2), are integrated in the same plot for further comparison. The simulation results of Fig. 4 compare favorably with that by Ursino [11] in the corresponding data range. In Fig. 5, we demonstrate the simulation results of the simulation module 5 with following initial parameters: r_m=0.027 cm, r_t=0.018 (cm), n_m=1.83, and T_{max}=2.16 (mmHg). The responses of Tm_1 (smooth muscle tension) vs. r_1 and Tm_2(wall thickness) vs. r_2 are shown in the left and middle portions of Fig. 5, respectively. In the right portion of Fig. 5, both smooth muscle tensionand radius of arteries, (Tm_1,

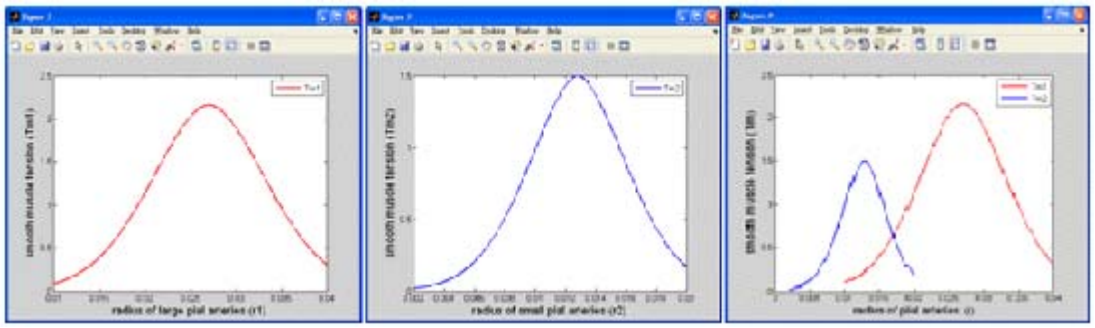

Fig. 5. Simulation of smooth muscle tension ($Tm_1$and Tm_2) vs. radius of large and small pial arteries (r_1 and r_2)

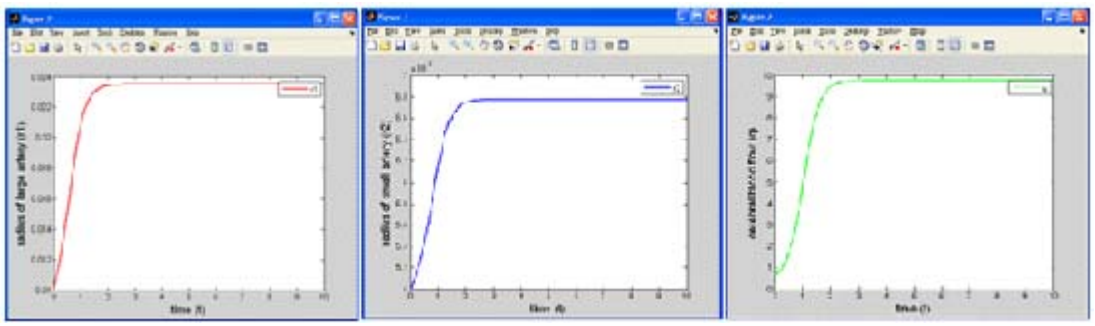

Fig. 6. The temporal responses of artery radius (r_1(t) and r_2(t)) and cerebral blood flow (q(t))

r_1) and (Tm_2, r_2), are integrated in the same plot for further comparison.

In Fig. 6, the temporal responses of the simulation module 7 with mean arterial pressure P_a=100 (mmHg) and mean cerebral capillary pressure P_{ic}=9.5 (mmHg) are presented. In the left and middle portions of Fig. 6, the variation of the radius of large (r_1(t)) and small pial arteries (r_2(t)) are depicted in time domain. In the right portion of Fig. 6, the simulation of cerebral blood flow in time domain (q(t)) is displayed. In comparison with those predicted in the model by Ursino and Giammarco [20], fewer magnitudes in variation of radius and cerebral blood flow are established in current simulator.

CONCLUSIONS

The objective of current study was aimed at establishing a numerical computation process and simulation tool for the study of cerebral autoregulation.We employed the electric analog of the arterial-arteriolar cerebrovascular bed proposed by Ursino [11]with description of blood dynamics and biomechanics from the viewpoints of both cerebral circulation and intracranial space for modeling and simulation. The CA simulator with intracranial dynamics, which equipped with seven simulation modules, was successfully implemented based on Matlab platform.With the simulation results show favourably agreement with neurological physiology and model behaviour of earlier researches, the implemented CA simulator provides fundamental but valuable tool in the discipline of biomedical engineering and cerebral autoregulation.

ACKNOWLEDGEMENT

This research was supported in part by the National Science Council, Taiwan, under grantnumber NSC 99-2221-E-035-053and NSC 101-2221-E-035-005.

REFERENCES

1. Lassen, N.A.,"Cerebral blood flow and oxygen consumption in man", *Physiol. Reviews*, 1959; **39**: 183-283.
2. Aaslid, R., K. Lindergaard, W.Sorteberg, H.Nornes , Cerebral autoregulation dynamics in humans. *Stroke*, 1989; **20**: .45-52.
3. Paulson, O.B., S.Strandgaard, L.Edvinsson, "Cerebral autoregulation. Cerebrovasc", *Brain Metab. Rev.,* 1990; **2**: 161-192.
4. Tiecks, F.P., A.M.Lam, R.Aaslid, D.W.Newell, "Comparison of static and dynamic cerebral autoregulation measurements", Stroke, 1995; **26:** 1014-1019.
5. Dawson, S.L.M.J.Blake, R.B.Panerai, J.F.Potter, "Dynamic but not static cerebral autoregulation is impaired in acute ischemic stroke", Cerebrovascular Diseases, 2000; **10**: 126-132.
6. Czosnyka, M., S.Piechnik, H.Richards, P.Kinesiatrics, P.Smileless, J.Pickard, "Contribution of mathematical modeling to the interpretation of the bedside tests of cerebrovascular autoregulation", *J. Neurol. Neurosurg Psychiatry,* 1997; **63**: 721-731.
7. Ursino, M., "A mathematical study of human intracranial hydrodynamics. Part 1: The cerebrospinal fluid pulse pressure", *Ann. Biomed. Eng*., 1988; **16**: 379-402.
8. Ursino, M.,"A mathematical study of human intracranial hydrodynamics. Part 2: Simulation of clinical tests", *Ann. Biomed. Eng*., 1988; **16**: 403-416.
9. Ursino M., P.D.Giammarco, E.Belardinelli,"A mathematical model of cerebral blood flow chemical regulation. Part I: Diffusion processes", IEEE *Trans. Biom. Eng*., 1989; **36**: 183-191.
10. Ursino, M., P.D.Giammarco, E.Belardinelli,"A mathematical model of cerebral blood flow chemical regulation. Part II: Reactivity of cerebral vascular bed", IEEE *Trans. Biom. Eng.,* 1989; **36**: 192-201.
11. Ursino, M., C.A.Lodi,"Interaction among autoregulation, CO_2 reactivity, and intracranial pressure: a mathematical model", *Am. J. Physiol. Heart Circ. Physiol.,* 1998; **274**: 1715-1728.
12. Ursino, M., E.Magosso,"Role of tissue hypoxia in cerebrovascular regulation: a mathematical modeling study", *Ann. Biomed. Eng*., 2001; **29**: 563-574.
13. Wang, D., C. Wang, "Real-time Visualization of Impact-Rotary Drill Simulator in Dynamic Terrain", JDCTA, 2012; **6**(8): .151-159.
14. Lin, S.L.,N.R. Guo, C.C. Chiu, "Modelling and Simulation of Respiratory Control with LabVIEW", *J. of Med. and Biolo. Eng.,* 2012; **32**(1): 51~60.
15. Yang, L., J. Sui, Y. Hu, X. Zhang, Y. Jin, "Cerebral Circulation Nonlinear Modeling and Vertebral Artery Stenosis Pathological Simulation", JCIT, 2011; **6**(11): 361-370.

16. Yang, L., J. Sui, Y. Hu, X. Zhang, Y. Jin, , "Cerebral Circulation Averaging Computation and Pathological Analysis", *IJACT*, 2011; **3**(11): 88-95.
17. Giannessi, M., M.Ursino, W. Murray, "The design of a digital cerebrovascular simulation model for teaching and research", *Anesth. Analg.,* 2008; **107**: 1997-2008.
18. Davis, M.J., R.W.Gore,"Length-tension relationship of vascular smooth muscle in single arterioles", *Am. J. Physiol. Heart Circ. Physiol.,* 1989; **256**: 630-640.
19. Traystman, R.J.,"The paper that completely altered our thinking about cerebral blood flow measurement", *J. Appl. Physiol.,* 2004; **97**: 1601-1602.
20. Ursino, M., P.D.Giammarco, "A mathematical model of the relationship between cerebral blood volume and intracranial pressure changes: the generation of plateau waves", *Ann. Biomed. Eng.,* 1991; 19: 15-42.